

# Preparation of Si<sub>3</sub>N<sub>4</sub> Foam Ceramics with Nest-Like Cell Structure by Particle-Stabilized Foams

Juanli Yu,<sup>‡</sup> Jinlong Yang,<sup>‡,†</sup> Sen Li,<sup>§</sup> Hexin Li,<sup>‡</sup> and Yong Huang<sup>‡</sup>

<sup>‡</sup>State Key Lab of New Ceramics and Fine Processing, Department of Materials Science and Engineering, Tsinghua University, Beijing 100084, China

<sup>§</sup>Institute of Mechanics, Chinese Academy of Sciences, No.15 Beisihuanxi Road, Beijing, China

Silicon nitride, Si<sub>3</sub>N<sub>4</sub> foam ceramics were prepared by particle-stabilized foams, and the stabilization of Si<sub>3</sub>N<sub>4</sub> foams and the performance of Si<sub>3</sub>N<sub>4</sub> foam ceramics were investigated. The Si<sub>3</sub>N<sub>4</sub> particle-stabilized foams had high stabilization, the dried green bodies had little shrinkage, and the structure of dried green body surface had no macro-pores and cracks. The Si<sub>3</sub>N<sub>4</sub> foam ceramics with nest-like cell structure were obtained, nest pores were jointed by elongated rod-shaped β-Si<sub>3</sub>N<sub>4</sub> grains with aspect ratio of 30 or so, pore distribution was uniform, the average pore size was about 16 μm, and the flexural strength was in the range of 3.8 to 77.2 MPa when porosity varied from 82.1% to 60.6%.

## I. Introduction

POROUS silicon nitride (Si<sub>3</sub>N<sub>4</sub>) ceramics have high porosity, high specific surface, low density, high hardness, low thermal expansion, and excellent corrosion resistance, and they can be widely applied in industrial applications, such as high temperature gas/liquid filters, catalyst supports, separation membranes, and thermal insulators.

In recent years, many researchers have investigated the preparation of porous Si<sub>3</sub>N<sub>4</sub> ceramics<sup>1–3</sup> by various processing routes, such as adding pore-forming agents,<sup>4</sup> direct foaming method,<sup>5</sup> the polymeric sponge impregnation,<sup>6</sup> freeze drying,<sup>7</sup> carbothermal nitridation of silica,<sup>8,9</sup> dual-phase mixing technique,<sup>10</sup> and gel casting.<sup>11,12</sup> Direct foaming method is an easy, cheap, and fast method for preparing highly porous ceramics with open or closed pores.<sup>13,14</sup> In the method, air bubbles are incorporated into a ceramic suspension to produce wet foams, wet foams are thermodynamically unstable because of their large air-water interfacial area and high overall free energy, and stabilization of foams is crucial to prepare high-performance porous ceramics. Surfactants are conventionally used to reduce the free energy of wet foams by adsorbing at the air bubble surface and reducing the air-water interfacial energy.

Recent researches on direct foaming method have found that the partially hydrophobic particles can attach to gas-liquid interfaces to stabilize air bubbles in surfactant-free diluted suspensions.<sup>15,16</sup> In the method, particles are used as foam stabilizers, their surfaces are modified by adsorbing short-chain amphiphilic organic molecules. As opposed to conventional surfactant molecules that adsorb and desorb on relatively short time scales,<sup>17,18</sup> the high stability of particle-stabilized foams in the wet state is attributed to the irrevers-

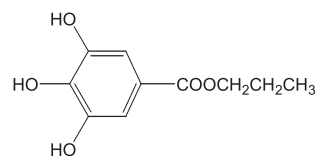
ible adsorption of the partially hydrophobic particles at the air-water interface.<sup>17–20</sup>

Although colloidal particles have been widely used for foam stabilization,<sup>21,22</sup> the study on Si<sub>3</sub>N<sub>4</sub> as colloidal particles for foam stabilization during direct foaming method has not been reported. In this article, the preparation of porous Si<sub>3</sub>N<sub>4</sub> ceramics by particle-stabilized foams is investigated, the stability of Si<sub>3</sub>N<sub>4</sub> particle-stabilized foams is studied, and the Si<sub>3</sub>N<sub>4</sub> foam ceramics with nest-like cell structure are obtained.

## II. Experimental Procedure

### (1) Materials

Silicon nitride, Si<sub>3</sub>N<sub>4</sub> powders (mean particle size 0.5 μm, α phase >94 wt%) employed in the experiment are commercially available materials. The sintering additives used are Al<sub>2</sub>O<sub>3</sub> (mean particle size 1.07 μm, 99% purity) and Y<sub>2</sub>O<sub>3</sub> (mean particle size: 4.74 μm, 99.9% purity) as. Powders of Si<sub>3</sub>N<sub>4</sub>, Al<sub>2</sub>O<sub>3</sub>, and Y<sub>2</sub>O<sub>3</sub> are all from Junyu Ceramic-molded Product Co., Ltd (Jing'an, Shanghai, China) Carboxymethyl cellulose (CMC; Sinopharm Chemical Reagent Co., Ltd., Shanghai, China) is used as the organic binder. Dispersant [1 wt%, ammonium salt of poly(acrylic acid)] is added to minimize agglomeration. In the study, the long-chain surfactants are octylphenol ethoxylate (TritonX-114, C<sub>34</sub>H<sub>62</sub>O<sub>11</sub>, AMRESCO Inc., Solon, OH), the short-chain amphiphilic molecules are propyl gallate (C<sub>10</sub>H<sub>12</sub>O<sub>5</sub>; Sinopharm Chemical Reagent Co., Ltd), and the chemical formula of propyl gallate is as follows:



Previous researches found that the particle surfaces were lyophobic through the adsorption of short amphiphiles via electrostatic interactions (carboxylates and amines) and ligand exchange reactions (gallates).<sup>23</sup> For the preparation of porous Si<sub>3</sub>N<sub>4</sub> ceramics by particle-stabilized foams, the selection of short-chain amphiphilic molecules depends on Zeta potential of Si<sub>3</sub>N<sub>4</sub> particles. Previous works suggested that propyl gallate has appropriate anchoring groups and pH conditions for Si<sub>3</sub>N<sub>4</sub> particle-stabilized foams.<sup>24</sup> In the study, samples for Zeta potential measurements are prepared at a solids concentration of 1.0 wt% in deionized water, dispersed for 30 min using an ultrasonic probe. After dispersing, the solution is allowed to sediment for 24 h and the agglomerates are removed. The measurements are performed at 25°C on Zetasizer to determine the Zeta potential as a function of pH, the 10<sup>-2</sup> N HCl and 10<sup>-2</sup> N NaOH solutions are used to adjust pH to the desired values. Figure 1

P. Colombo—contributing editor

Manuscript No. 30129. Received August 07, 2011; approved November 16, 2011.

<sup>†</sup>Author to whom correspondence should be addressed. e-mail: yujuanli@126.com

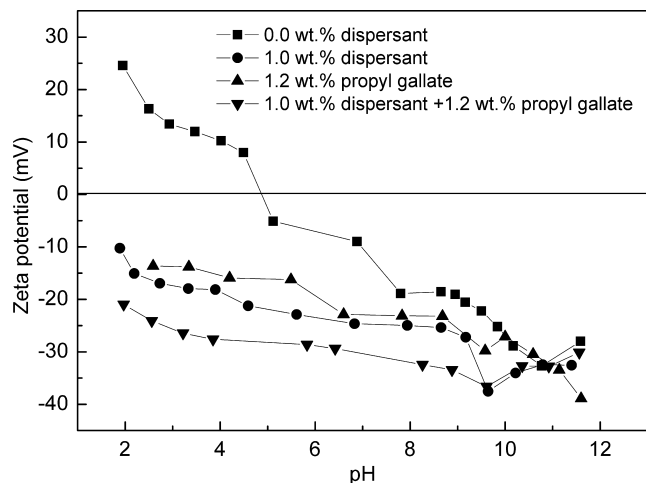


Fig. 1. Zeta potential as a function of pH for  $\text{Si}_3\text{N}_4$  particles.

shows the effects of the additions of dispersant and propyl gallate on Zeta potential of  $\text{Si}_3\text{N}_4$  particles at different pH values, and it indicates that the maximal absolute value of Zeta potential of  $\text{Si}_3\text{N}_4$  particles with the additions of dispersant and propyl gallate is achieved at pH 9.5. In Fig. 1, the variations of Zeta potentials of  $\text{Si}_3\text{N}_4$  particles with pH are similar for dispersant addition and propyl gallate addition, Zeta potentials keep negative in the whole range of pH (2–12), and this indirectly indicates that propyl gallate can effectively absorb on the surfaces of  $\text{Si}_3\text{N}_4$  particle as a dispersant does.

## (2) Processing and Characterization

During the preparation of porous  $\text{Si}_3\text{N}_4$  ceramics by particle-stabilized foams, in the first step, carboxymethyl cellulose (CMC) (1 wt%, based on deionized water) and ammonium salt of poly(acrylic acid) as dispersant (1 wt%, based on silicon nitride powder) are completely dissolved in deionized water by mechanical stirring. The next step is to add  $\alpha\text{-Si}_3\text{N}_4$  powders with 6 wt% sintering additives (2 wt%,  $\text{Al}_2\text{O}_3$ ; 4 wt%,  $\text{Y}_2\text{O}_3$ , based on silicon nitride powder) into the premix solution, ammonia aqueous is used to adjust pH to 9.5 and the mixture is rolled for 12 h, followed by the gradual addition of dissolved propyl gallate/TritonX-114 (1.2 wt%, based on silicon nitride powder), the suspension foaming is carried out using a household mixer at full speed for 5–10 min, then thick foam is cast immediately into a suitable mold and foam drying is subsequently carried out

in air. Finally, under nitrogen atmosphere (0.1–0.9 MPa), sintering is performed at a heating rate of  $10^\circ\text{C}/\text{min}$  and 1.5–4 h holding time at  $1750^\circ\text{C}$ , and then sintered  $\text{Si}_3\text{N}_4$  foam ceramics is achieved.

Samples for Zeta potential measurements are performed at  $25^\circ\text{C}$  on Zetasizer (3000HS; Brookhaven Corp., Upton, NY). The microstructures of  $\text{Si}_3\text{N}_4$  foam ceramics are observed using scanning electron microscopy (SEM; S-570, Hitachi, Ltd., Tokyo, Japan). The porosity of the sintered body is measured using the Archimedes displacement technique. Phase analysis is conducted by X-ray diffraction (XRD) via a computer controlled diffractometer (XRD; XRD-6000, Shimadzu Corp., Kyoto, Japan). Pore-size distribution of the sintered body is measured using mercury porosimetry (AutoPore IV 9510, Micromeritics Instrument Corp., Norcross, GA).

The room-temperature flexural strengths of sintered  $\text{Si}_3\text{N}_4$  foam ceramics are determined by three-point flexural test. The specimens are machined into test bars of  $30\text{ mm} \times 4\text{ mm} \times 3\text{ mm}$ , and the three-point flexural strength is measured on specimen bars of a span of 16 mm at a crosshead speed of  $0.5\text{ mm}/\text{min}$  (Instron 1195; Instron Corp., Dallas, TX). The flexural strength ( $\sigma_f$ ) is determined by the standard equation:

$$\sigma_f = (3PL)/(2bh^2) \quad (1)$$

where  $P$  is the fracture load;  $L$  is the length of support span;  $b$  is the specimen width;  $h$  is the specimen thickness. By repeating the tests for porous silicon nitride five times for each specimen, the results are given as the mean values of five measurements.

## III. Results and Discussion

### (1) Stability of $\text{Si}_3\text{N}_4$ Particle-Stabilized Foam

Since the pores of foam ceramics prepared by direct foaming method mainly originate from the foams, the stability of the foams is crucial to the performance of foam ceramics. To investigate the foam stability, the variations of foams in graduated cylinder with holding time are observed.

Figure 2 shows the foam stability and the dried large size ceramic foams. Figure 2(a) compares the foam stability of conventional surfactant molecules stabilized ceramic foams and ceramic particle-stabilized foams. The height variation of ceramic foams prepared by conventional surfactant molecules stabilized foams in a graduated cylinder for 3 h holding time, the collapse height rate is 70% or so, the collapse of foam is very distinct, and it indicates that the foam is unstable. The height

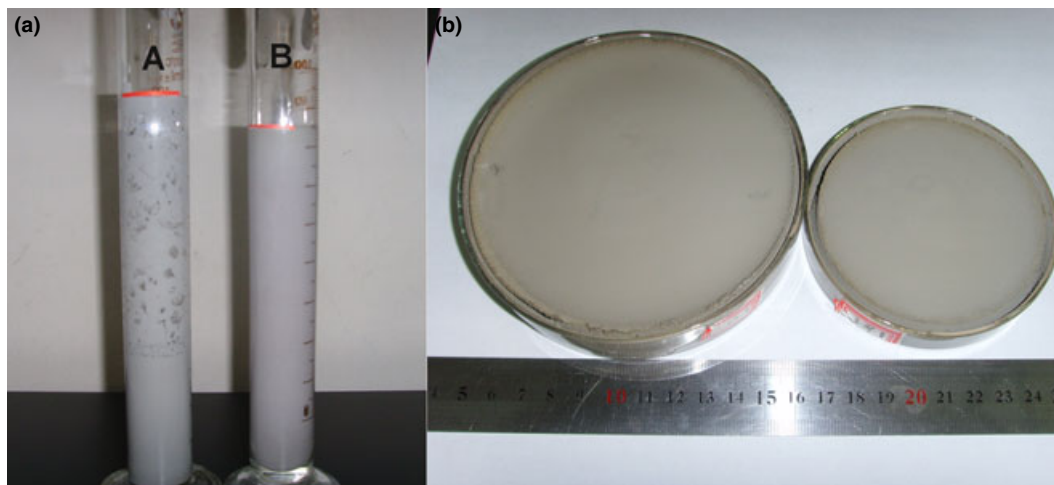


Fig. 2. Foam stability and the dried large size ceramic foams (a) the comparison of foam stability: (A) surfactant molecules (TritonX-114) stabilized foam, (B) particle-stabilized foam; (b) the dried large size ceramic foams obtained by particle-stabilized foam.

variation of foam prepared by particle-stabilized foams in a graduated cylinder for 48 h holding time, there is no collapse, and this indicates that the foam prepared by particle-stabilized foam is stable. The long-chain surfactants cannot prevent the long-term destabilization of foams due to the low adsorption energy of surfactants at the gas-liquid interface, and the wet foams stabilized with long-chain surfactants coarsen or collapse within a few minutes after foaming. For wet foams prepared by particle-stabilized foam, particles can adsorb on the surface of gas bubbles to stabilize the gas-liquid interface, particles lower the overall free energy of the system by replacing part of the high-energetic gas-liquid interfacial area with less energetic interfaces. Particles adsorbed at the interface impede bubble coalescence and form an interfacial armor that hinders gas diffusion outside the bubble, and thus particle-stabilized foams exhibit enhanced stability in comparison with foams stabilized by surfactants.<sup>25</sup>

During the drying of wet green body prepared by  $\text{Si}_3\text{N}_4$  particle-stabilized foam, the shrinkage and crack affect the performance of ceramic. Figure 2(b) shows that the dried large size ceramic foams have little shrinkage by particle-stabilized foam during drying in air, and the structure of dried foam surface is uniform and has no macro-pores and cracks. High stability of  $\text{Si}_3\text{N}_4$  particle-stabilized foam makes the structure of wet foams uniform, then dried green body has little shrinkage and the surface no crack, and thus it is conducive to prepare high-performance foam ceramics.

## (2) Development of Microstructures in $\text{Si}_3\text{N}_4$ Foam Ceramics

Figure 3 shows the XRD profiles of  $\text{Si}_3\text{N}_4$  foam ceramics, and the results indicate that the  $\alpha$ - $\beta$  transformation at temperature of 1680°C is incomplete where a large amount of  $\alpha$ - $\text{Si}_3\text{N}_4$  remains in the sample, the formation of  $\beta$ - $\text{Si}_3\text{N}_4$  is enhanced when heating up to higher temperature, and heating to 1750°C directly results in the formation of  $\beta$ - $\text{Si}_3\text{N}_4$  single phase.

The  $\alpha \rightarrow \beta$ - $\text{Si}_3\text{N}_4$  phase transformation is of a reconstructive nature via a solution-reprecipitation mechanism. Extensive studies have been made to determine the kinetics and mechanisms of the  $\alpha$ - $\beta$  transformation,<sup>26,27</sup> and the flowchart of the formation process of the microstructure is shown in Fig. 4. The  $\alpha$ - $\text{Si}_3\text{N}_4$  grains are equiaxed, which is metastable during sintering (e.g., at 1400°C–2000°C and 0.1–100 MPa  $\text{N}_2$  pressure),<sup>28</sup>  $\alpha$ - $\text{Si}_3\text{N}_4$  grains transform irreversibly to elongated

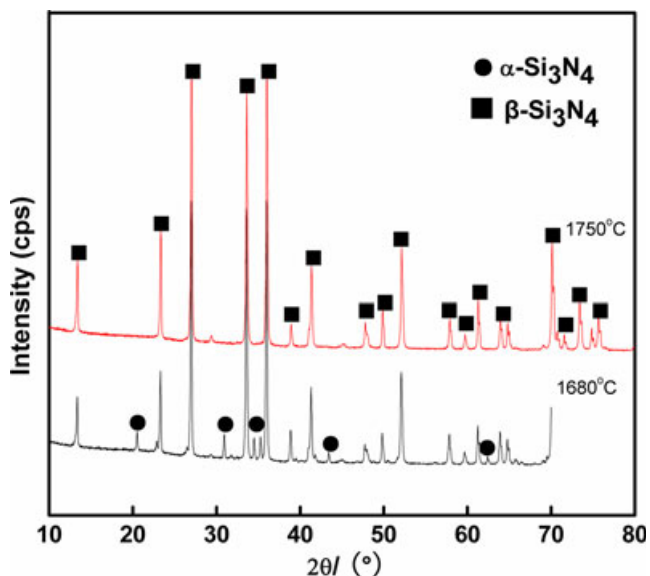


Fig. 3. XRD patterns of  $\text{Si}_3\text{N}_4$  foam ceramics sintered at different temperature holding for 1 h.

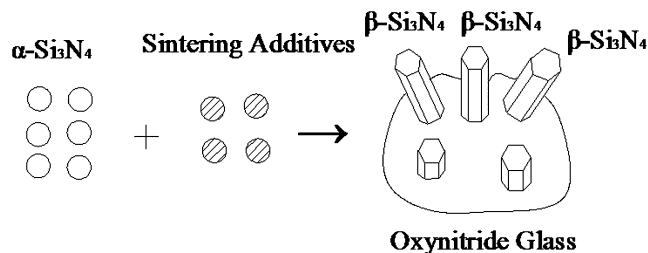


Fig. 4. Schematic representation of the formation process of  $\text{Si}_3\text{N}_4$  microstructure.<sup>29</sup>

$\beta$ - $\text{Si}_3\text{N}_4$  grains, and the elongated  $\beta$ - $\text{Si}_3\text{N}_4$  grains are formed *in situ* through a solution-precipitation process in the presence of a liquid phase of sintering additives.<sup>29,30</sup> The obtained  $\text{Si}_3\text{N}_4$  cannot be densified by common dry sintering, the addition of sintering aids to create a liquid-phase sintering process is necessary because of its covalent bonding and low diffusivity, and the liquid phase accelerates the  $\alpha$ - $\text{Si}_3\text{N}_4$  to  $\beta$ - $\text{Si}_3\text{N}_4$  transformation and crystal growth, as shown in Fig. 4. The microstructural development of  $\text{Si}_3\text{N}_4$  ceramics is controlled mainly by the  $\text{Si}_3\text{N}_4$  starting powders, the additives, and the sintering parameters.<sup>28,31–35</sup>

To obtain the  $\text{Si}_3\text{N}_4$  foam ceramics with nest-like cell structure, the sintering nitrogen pressure and holding time are adjusted at temperature 1750°C, the  $\text{Si}_3\text{N}_4$  foam ceramics with nest-like cell structure are achieved, and the SEM micrographs of  $\text{Si}_3\text{N}_4$  foam ceramics are shown in Figs. 5 and 6.

Figure 5 shows the nest-like microstructures of  $\text{Si}_3\text{N}_4$  foam ceramics sintered at nitrogen pressure of 0.1 MPa and 1.5 h holding time at 1750°C. The pores are relatively uniform, small, and spherical [see Fig. 5(a)]. The nest-like microstructure with elongated rod-shaped  $\beta$ - $\text{Si}_3\text{N}_4$  grains is exhibited in every pore cell [see Fig. 5(b)], most of the elongated rod-shaped  $\beta$ - $\text{Si}_3\text{N}_4$  grains inside the pores have high aspect ratio (the ratio of grain length to thickness or diameter), the length of the elongated rod-shaped  $\beta$ - $\text{Si}_3\text{N}_4$  grain is about 16.0  $\mu\text{m}$ , the diameter is about 571 nm, and the aspect ratio is 30 or so [see Fig. 5(c)].

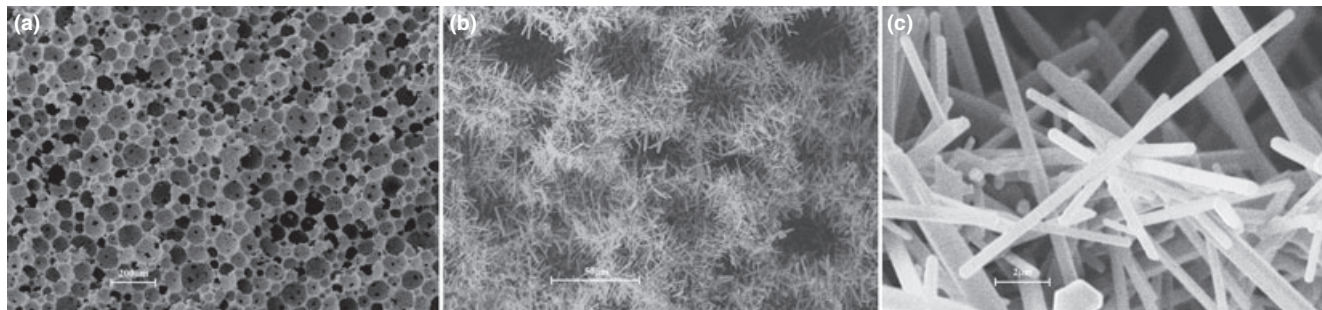
Figure 6 shows the nest-like microstructures of  $\text{Si}_3\text{N}_4$  foam ceramics sintered at nitrogen pressure of 0.9 MPa and 4 h holding time at 1750°C. The nest-like microstructure with elongated rod-shaped  $\beta$ - $\text{Si}_3\text{N}_4$  grains is exhibited in every pore cells [see Figs. 6(a) and (b)]. The length of the elongated rod-shaped  $\beta$ - $\text{Si}_3\text{N}_4$  grains is 22.2  $\mu\text{m}$ , with diameter of about 1.47  $\mu\text{m}$  and the aspect ratio is about 15.1 or less [see Fig. 6(c)].

The comparison of Figs. 5 and 6 indicates that, with the increase of nitrogen pressure and holding time during sintering, the growth rate of the  $\beta$ - $\text{Si}_3\text{N}_4$  grains diameter is higher than that of the length, and the aspect ratio decreases. Similar tendencies were reported in other investigations<sup>36,37</sup> and theoretically predicted by modeling studies.<sup>38</sup>

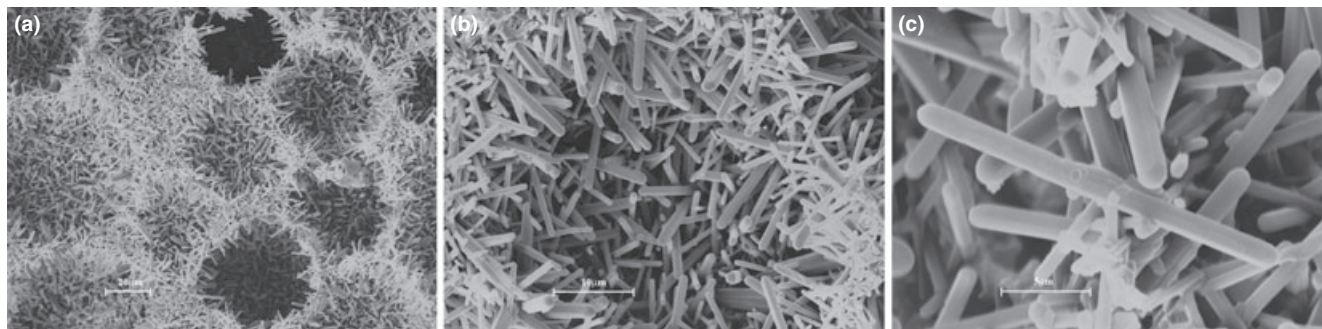
## (3) The Properties of $\text{Si}_3\text{N}_4$ Foam Ceramics with Nest-Like Microstructure

Figure 7 shows the pore-size distribution of  $\text{Si}_3\text{N}_4$  foam ceramics with nest-like structure presented in Fig. 5. The average pore size shown here is about 16  $\mu\text{m}$ . The pores have an almost sharp distribution, and it means that pore distribution is very uniform (see Figs. 5 and 6). The uniform pore distribution originates from the uniform structure of green body, and the uniform structure of  $\text{Si}_3\text{N}_4$  particle-stabilized foams can effectively improve the performance of foam ceramics.

To investigate the relationship between mechanical property and porosity of  $\text{Si}_3\text{N}_4$  foam ceramics with nest-like structure, the foaming rate is adjusted to change the porosity of  $\text{Si}_3\text{N}_4$  foam ceramics in the preparation of  $\text{Si}_3\text{N}_4$  foam



**Fig. 5.** The microstructures of sintered  $\text{Si}_3\text{N}_4$  foam ceramics at nitrogen pressure of 0.1 MPa and 1.5 h holding time at 1750°C. (a) the uniformity of pores with nest-like cell structure, (b) the presence of nest-like structure in every cell, (c) the single elongated rod-shaped  $\beta\text{-Si}_3\text{N}_4$  grain.



**Fig. 6.** The microstructures of sintered  $\text{Si}_3\text{N}_4$  foam ceramics at nitrogen pressure of 0.9 MPa, 4 h holding time at 1750°C. (a) the presence of nest-like structure in every cell, (b) the elongated rod-shaped  $\beta\text{-Si}_3\text{N}_4$  in the pore cells, (c) the single elongated rod-shaped  $\beta\text{-Si}_3\text{N}_4$  grain.

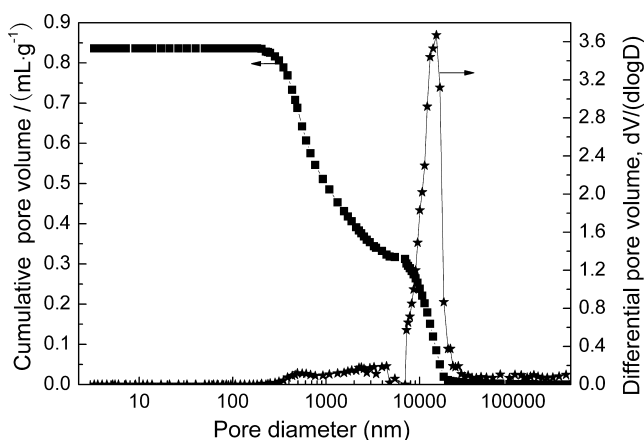


**Fig. 7.** Pore size distribution of sintered  $\text{Si}_3\text{N}_4$  foam ceramics at nitrogen pressure of 0.1 MPa and 1.5 h holding time at 1750°C.

ceramics by controlling the concentration of amphiphilic molecules and the solid loading, as shown in Table I. The foaming rate increases with the increase of concentration of amphiphilic molecules, but it decreases with the increase of solid loading.

The influence of the porosity on flexural strength is shown in Fig. 8. The results indicate that flexural strength monotonically decreases with the increase of porosity, the flexural strength is in the range of 3.8 to 77.2 MPa when porosity varies from 82.1% to 60.6%. Tuyen<sup>33</sup> prepared  $\text{Si}_3\text{N}_4$  foam ceramics by pressure sintered (GPSed)-reaction bonded silicon nitride process, pore size was about 300  $\mu\text{m}$ , and the flexural strength was not reported. Normally, the large pores (e.g., 300  $\mu\text{m}$ ) in foam ceramics significantly reduce the mechanical strength. Shao<sup>39</sup> prepared silicon nitride/silicon oxynitride ( $\text{Si}_3\text{N}_4/\text{Si}_2\text{N}_2\text{O}$ ) foam ceramics by gelcasting technique, the bending strength varied from 21 to

**Table I.** The Influences of Concentration of Amphiphilic Molecules and Solid Loading on Foaming Rate

Solid loadings (vol%)	Amphiphiles (g/L)	Foaming rate (vol%)
25	6.4	63.2
25	9.5	65.0
25	12.7	70.9
25	15.9	76.2
25	21.2	78.1
45	6.4	43.2
45	9.5	53.3
45	12.7	59.0
45	15.9	61.5
45	21.2	65.3

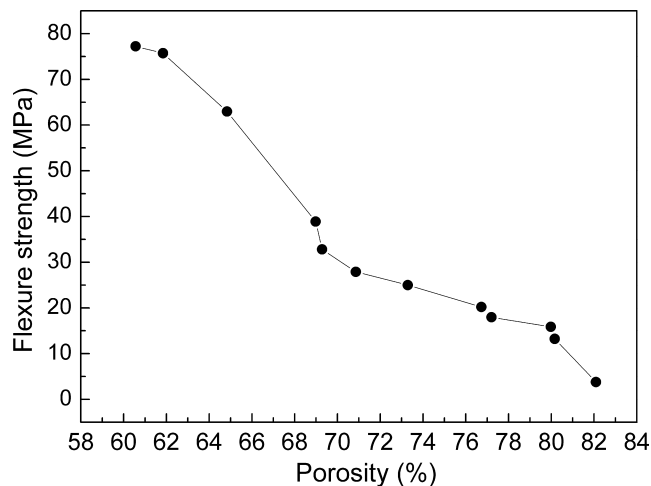


**Fig. 8.** Flexural strength as functions of porosity.

39 MPa when the porosity was in the range 67.4%–62.0%, and pore size was about 200  $\mu\text{m}$ . In the study, the pore size of high stable particle-stabilized foams can be effectively controlled by adjusting solid loading and foaming rate, and the average pore size of  $\text{Si}_3\text{N}_4$  foam ceramics prepared by particle-stabilized foams is only 16  $\mu\text{m}$ , this improves the mechanical property of  $\text{Si}_3\text{N}_4$  foam ceramics, and thus 77.2 MPa of the flexural strength can be achieved when the porosity is 60.6%.

#### IV. Conclusions

Porous  $\text{Si}_3\text{N}_4$  ceramics were prepared by particle-stabilized foams. Particle-stabilized foams were more stable than the conventional foams, the dried green body had little shrinkage by particle-stabilized foam, and the structure of dried foam surface was uniform and had no macro-pores and cracks. The microstructure of  $\text{Si}_3\text{N}_4$  foam ceramics is nest-like, nest pores are jointed by elongated rod-shaped  $\beta\text{-Si}_3\text{N}_4$  grains, the aspect ratio of the elongated rod-shaped  $\beta\text{-Si}_3\text{N}_4$  grain is about 30 or so. The pore distribution of  $\text{Si}_3\text{N}_4$  foam ceramics with elongated rod-shaped  $\beta\text{-Si}_3\text{N}_4$  grains is uniform, the average pore size is about 16  $\mu\text{m}$ , and the flexural strength is in the range of 3.8 to 77.2 MPa when porosity varies from 82.1% to 60.6%.

#### Acknowledgments

Our research work presented in this article is supported by the National High Technology Research and Development Program of China (Grant No 2010AA03A408), and Beijing Sci-tech Plan of China (Grant No 20101092117). The authors are grateful for these grants.

#### References

- J. F. Yang and S. A. Diaz, "Microstructure and Mechanical Properties of Silicon Nitride Ceramics with Controlled Porosity," *J. Am. Ceram. Soc.*, **85** [6] 1512–6 (2002).
- T. Ohji, "Microstructural Design and Mechanical Properties of Porous Silicon Nitride Ceramics," *Mater. Sci. Eng. A*, **498** [1/2] 5–11 (2008).
- J. L. Yu, H. J. Wang, and H. Zeng, *et al.* "Investigation on Gel Casting Preparation of Porous Silicon Nitride Ceramics Through Orthogonal Experimental Design," *Mater. Sci. Forum*, **569**, 49–52 (2008).
- O. Lyckfeldt and J. M. F. Ferreira, "Processing of Porous Ceramics by "Starch Consolidation"," *J. Eur. Ceram. Soc.*, **18** [2] 131–40 (1998).
- J. L. Yu, J. L. Yang, and Y. Huang, *et al.* "Study on Particle-Stabilized  $\text{Si}_3\text{N}_4$  Ceramic Foams," *Mater. Lett.*, **65** [12] 1801–4 (2011).
- L. L. Wood, P. Messina, and K. C. Frisch, "Method of Preparing Porous Ceramic Structures by Firing a Polyurethane Foam That is Impregnated with Inorganic Materials," US Patent No. 3833386, 1974-9-3.
- T. Fukasawa, Z. Y. Deng, and M. Ando, "Synthesis of Porous Silicon Nitride with Unidirectionally Aligned Channels Using Freeze-Drying Process," *J. Am. Ceram. Soc.*, **85** [9] 2151–5 (2002).
- Y. Zhang, H. J. Wang, and Z. H. Jin, "Preparation and Study of Porous  $\text{Si}_3\text{N}_4$  Ceramics with High Strength," *Rare Metal Mater. Eng.*, **33** [6] 655–8 (2004).
- W. Zhang, H. J. Wang, and Z. H. Jin, *et al.* "Preparation and Properties of Macroporous Silicon Nitride Ceramics by Gelcasting and Carbon Thermal Reaction," *J. Mater. Sci. Technol.*, **21** [4] 894–8 (2005).
- J. F. Yang, G. J. Zhang, and N. Kondo, *et al.* "Synthesis of Porous  $\text{Si}_3\text{N}_4$  Ceramics with Rod-Shaped Pore Structure," *J. Am. Ceram. Soc.*, **88** (4), 1030–2 (2005).
- J. L. Yu, H. J. Wang, and J. Zhang, *et al.* "Gelcasting Preparation of Porous Silicon Nitride Ceramics by Adjusting the Content of Monomers," *J. Sol-Gel. Sci. Technol.*, **53** [3] 515–23 (2010).
- J. L. Yu, H. J. Wang, and H. Zeng, *et al.* "Effect of Monomer Content on Physical Properties of Silicon Nitride Ceramic Green Body Prepared by Gelcasting," *Ceram. Int.*, **35** [3] 1039–44 (2009).

- A. R. Studart, U. T. Gonzenbach, E. Tervoort, and L. J. Gauckler, "Processing Routes to Macroporous Ceramics: A Review," *J. Am. Ceram. Soc.*, **99** [6] 1771–89 (2006).
- P. Sepulveda and J. G. P. Binne, "Processing of Cellular Ceramics by Foaming and In-Situ Polymerisation of Organic Monomers," *J. Eur. Ceram. Soc.*, **19** [12] 2059–66 (1999).
- B. P. Binks, "Particles as Surfactants-Similarities and Differences," *Curr. Opin. Colloid Interface Sci.*, **7** [1–2] 21–41 (2002).
- Z. P. Du, M. P. Bilbao-Montoya, and B. P. Binks, *et al.* "Outstanding Stability of Particle-Stabilized Bubbles," *Langmuir*, **19** [8] 3106–8 (2003).
- U. T. Gonzenbach, A. Studart, and E. Tervoort, *et al.* "Stabilization of Foams with Inorganic Colloidal Particles," *Langmuir*, **22** [6] 10983–8 (2006).
- I. Akartuna, A. Studart, and E. Tervoort, *et al.* "Stabilization of Oil-in-Water Emulsions by Colloidal Particles Modified with Short Amphiphiles," *Langmuir*, **24** [14] 7161–8 (2008).
- A. R. Studart, U. T. Gonzenbach, E. Tervoort, and L. J. Gauckler, "Materials from Foams and Emulsions Stabilized by Colloidal Particles," *J. Mater. Chem.*, **17** [31] 3283–9 (2007).
- U. T. Gonzenbach, A. R. Studart, and D. Steinlin, *et al.* "Processing of Particle-Stabilized Wet Foams into Porous Ceramics," *J. Am. Ceram. Soc.*, **90** [11] 3407–14 (2007).
- S. Mishra, R. Mitra, and M. Vijayakumar, "Processing and Microstructure of Particle Stabilized Silica Foams," *Mater. Lett.*, **63** [30] 2649–51 (2009).
- J. L. Yang, H. Lin, X. Q. Xi, and K. Zeng, "Porous Ceramic from Particle Stabilized Foams by Gelcasting," *Int. J. Mater. Prod. Technol.*, **37** [3/4] 248–56 (2010).
- P. C. Hidber, T. J. Graule, and L. J. Gauckler, "Influence of the Dispersant Structure on Properties of Electrostatically Stabilised Aqueous Alumina Suspensions," *J. Eur. Ceram. Soc.*, **17** [2/3] 239–49 (1997).
- U. T. Gonzenbach, "Particle-Stabilized Foams"; A dissertation submitted to the Swiss Federal Institute of Technology Zürich for the degree of doctor of science, Zürich, pp. 53–4, 2006.
- U. T. Gonzenbach, A. R. Studart, and L. J. Gauckler, "Tailoring the Microstructure of Particle-Stabilized Wet Foams," *Langmuir*, **23** [3] 1025–32 (2007).
- C. M. Wang, X. Pan, and M. Rühle, "Review: Silicon Nitride Crystal Structure and Observations of Lattice Defects," *J. Mater. Sci.*, **31** [20] 5281–98 (1996).
- L. J. Bowen, T. G. Carruthers, and R. J. Brook, "Hot-Pressing of  $\text{Si}_3\text{N}_4$  with  $\text{Y}_2\text{O}_3$  and  $\text{Li}_2\text{O}$  Additives," *J. Am. Ceram. Soc.*, **61** [7–8] 335–9 (1978).
- G. Petzow, and M. Herrmann, "Silicon Nitride Ceramics"; pp. 47–167 in *High Performance Non-oxide Ceramics II: Structure and Bonding*, Vol. 102, Edited by M. A. Jansen and R. Haubner, Springer-Verlag, Berlin, Heidelberg, 2002.
- M. J. Hoffmann, P. F. Becher, and G. Petzow (eds) (1994) *Silicon Nitride 93-Proc Int Conf on Silicon Nitride-Based Ceramics*, Stuttgart Trans Tech Publications Ltd, Aedermannsdorf, Switzerland.
- T. Hirata, K. Akiyama, and T. Morimoto, "Synthesis of  $\beta\text{-Si}_3\text{N}_4$  Particles from  $\alpha\text{-Si}_3\text{N}_4$  Particles," *J. Eur. Ceram. Soc.*, **20** [8] 1191–5 (2000).
- D. Y. Chen, B. L. Zhang, and H. R. Zhuang, "Preparation and Growth Mechanism of  $\beta\text{-Si}_3\text{N}_4$  Rod-Like Crystals by Combustion Synthesis," *Mater. Lett.*, **57** [2] 399–402 (2002).
- P. F. Becher, G. S. Painter, and N. Shibata, "Influence of Additives on Anisotropic Grain Growth in Silicon Nitride Ceramics," *Mater. Sci. Eng. A*, **422** [1–2] 85–91 (2006).
- D. V. Tuyen, J. H. Yoo, and H. D. Kim, "Fabrication of  $\beta\text{-Si}_3\text{N}_4$  Whiskers from a GPSed-RBSN Sponge Using  $6\text{Y}_2\text{O}_3\text{-}2\text{MgO}$  Additives," *Ceram. Int.*, **36** [8] 2427–30 (2010).
- H. Emoto and M. Mitomo, "Control and Characterization of Abnormally Grown Grains in Silicon Nitride Ceramics," *J. Eur. Ceram. Soc.*, **17** [6] 797–804 (1997).
- E. Tani, "Gas-Pressure Sintering of  $\text{Si}_3\text{N}_4$  with Concurrent Addition of  $\text{Al}_2\text{O}_3$  and 5wt% Rare Earth Oxide: High Fracture Toughness  $\text{Si}_3\text{N}_4$  with Fiber-Like Structure," *Am. Ceram. Soc. Bull.*, **65** [9] 1311–5 (1986).
- M. Kitayama, K. Hirao, and M. Toriyama, "Control of  $\beta\text{-Si}_3\text{N}_4$  Crystal Morphology and its Mechanisms (Part1). Effect of  $\text{SiO}_2$  and  $\text{Y}_2\text{O}_3$  Ratio," *J. Ceram. Soc. Jpn.*, **107** [10] 930–4 (1999).
- L. A. Genova, V. A. Izhevskiy, and J. C. Bressiani, "Effect of Processing Variables on Synthesis of  $\beta\text{-Si}_3\text{N}_4$  Particles," *J. Eur. Ceram. Soc.*, **28** [3] 295–301 (2008).
- M. Kitayama, K. Hirao, and M. Toriyama, "Modeling and Simulation of Grain Growth in  $\text{Si}_3\text{N}_4$ . I: Anisotropic Ostwald Ripening," *Acta Mater.*, **46** [18] 6541–50 (1998).
- Y. F. Shao, D. C. Jia, Y. Zhou, and B. Y. Liu, "Novel Method for Fly Ash Cenosphere as a Pore-Forming Agent," *J. Am. Ceram. Soc.*, **91** [11] 3781–5 (2008). □